Similarity Measure Using Local Phase Features and Its Application to Biometric Recognition

Shoichiro Aoyama, Koichi Ito, Takafumi Aoki
Graduate School of Information Sciences, Tohoku University
6-6-05, Aramaki Aza Aoba, Aoba-ku, Sendai-shi, 980-8579, Japan
aoyama@aoki.ecei.tohoku.ac.jp

Abstract

In the field of biometric recognition, similarity measure using local features such as Gabor-based coding, Local Binary Patterns (LBP) and Scale Invariant Feature Transform (SIFT) has been applied to various biometric recognition problems. These features, however, may not always exhibit higher recognition performance than the recognition algorithms of the specific biometric trait. In this paper, we propose a novel similarity measurement technique using local phase features for biometric recognition. The phase information obtained from 2D Discrete Fourier Transform (DFT) of images exhibits good performance for evaluating the similarity between images. The local phase features extracted from multi-scale image pyramids can handle nonlinear deformation of images. Through a set of experiments in some biometric recognition such as face, palmprint and finger knuckle recognition, we demonstrate the efficient performance and versatility of the proposed features compared with the state-of-the-art conventional algorithms.

1. Introduction

Similarity measurement techniques based on local features have been used in biometric recognition problems. In the case of biometric recognition, the target to be recognized is limited to the biometric trait. We can normalize scale, rotation, translation, sometimes deformation and illumination of images depending on the target biometric trait in advance. Therefore, it is more important for local features to include the inherent information of the target biometric trait in order to measure the similarity between images.

Minutiae for fingerprint recognition can be considered as local features which consist of location, angle, type, etc. An iriscode for iris recognition [8] and a palmcode for palmprint recognition [28] are local features which are based on binary codes obtained by binarizing an image after Gabor filtering. Recently, Local Binary Patterns (LBPs) have been proposed [22] and been used as general-purpose local features for biometric recognition [1]. Scale Invariant Feature Transform (SIFT) [16], which is one of the famous local features in the field of computer vision, has also been applied to many biometric recognition problems [4, 17, 6, 20]. The similarity between images is then evaluated by the distance between local features.

The Gabor-based coding method has exhibited good performance in iris recognition [8] and in palmprint recognition [28]. The Gabor filter extracts the inherent texture information from images according to parameters of the filter kernel. Since the biometric traits have wrinkle patterns such as fingerprint, it is suitable for biometric recognition to extract features by using the Gabor filter optimized to each biometric trait. Recently, improved versions of Gabor-based method have been proposed and been applied to palmprint recognition [12, 33] and finger knuckle recognition [15, 31]. However, the recognition performance of Gabor-based coding methods is significantly dropped for deformed images, since these methods assume that images are completely aligned. Also, the parameters of Gabor filter have to be optimized depending on biometric traits and environmental factors of image acquisition.

The LBP-based method has been receiving much attention since its effectiveness has been demonstrated in face recognition [1]. LBP is obtained by thresholding neighborhoods of each pixel with the center pixel value, and then the histogram of LBPs is used as a texture descriptor. So far, the improved versions of LBP-based method have been proposed and been applied to various biometric recognition problems [5, 21, 18, 14]. LBP has the versatility for image matching since LBP dose not need any optimization process. On the other hand, LBP cannot handle large deformation of images and also may not exhibit the comparable performance with the other methods specified to each biometric trait due to its versatility.

The SIFT-based method has been applied to fingerprint recognition [23], face recognition [4, 17], palmprint recog-

nition [6] and finger knuckle recognition [20]. Using the property of SIFT such as robustness against geometric transformation, the number of corresponding point pairs can be used as similarity measure. On the other hand, for low-quality images, the recognition performance of SIFT-based methods may decrease, since SIFT keypoints extracted from low-quality images are sparse or partial.

Addressing the above problems, we consider to employ phase information obtained by Discrete Fourier Transform (DFT) of images, which is successfully applied to image matching tasks [26]. In particular, the phase-based image matching for biometric recognition called Band-Limited Phase-Only Correlation (BLPOC) has been proposed [11] and been used in various biometric recognition algorithms [9, 19, 29]. These algorithms cannot handle the nonlinear deformation of images, since the phase information obtained from the entire image is employed. To deal with nonlinear deformation, the approach combined with phase-based correspondence matching [27] and BLPOC has been proposed [10, 2]. This approach improves the recognition performance of biometric recognition, while the phase-based correspondence matching method is designed for computer vision problems and the large amount of data has to be registered in the database compared with other local features.

In this paper, we propose local phase features extracted from each layer of multi-scale image pyramids, which are designed specifically for biometric recognition. Using the proposed local phase features, we can align the global translation between images in the top layer, align the minute translation between local block images in the middle layer, and finally evaluate the similarity between local block images in the bottom layer. The amount of local phase features can also be reduced by phase quantization without sacrificing the performance of biometric recognition. We evaluate the performance and versatility of the proposed features thorough a set of experiments in face recognition, palmprint recognition and finger knuckle recognition.

2. Local Phase Features

This section describes the hierarchical local phase features proposed in this paper. We briefly introduce the fundamentals of phase-based image matching [26, 11], and then explain the details of the proposed local features.

2.1. Phase-Based Image Matching

We introduce the principle of a Phase-Only Correlation (POC) function (which is sometimes called the "phase-correlation function") [13, 7, 26].

Consider two $N_1 \times N_2$ images, $f(n_1, n_2)$ and $g(n_1, n_2)$, where we assume that the index ranges are $n_1 = -M_1, \cdots, M_1$ ($M_1 > 0$) and $n_2 = -M_2, \cdots, M_2$ ($M_2 > 0$) for mathematical simplicity, and hence $N_1 = 2M_1 + 1$ and $N_2 = 2M_2 + 1$. The discussion could be easily generalized to non-negative index ranges with power-of-two image size. Let $F(k_1, k_2)$ and $G(k_1, k_2)$ denote the 2D DFTs of the two images. $F(k_1, k_2)$ and $G(k_1, k_2)$ are given by

$$\begin{aligned} F(k_1, k_2) &= \sum_{n_1, n_2} f(n_1, n_2) W_{N_1}^{k_1 n_1} W_{N_2}^{k_2 n_2} \\ &= A_F(k_1, k_2) e^{j\theta_F(k_1, k_2)}, \end{aligned} \tag{1}$$

$$\begin{aligned} G(k_1, k_2) &= \sum_{n_1, n_2} g(n_1, n_2) W_{N_1}^{k_1 n_1} W_{N_2}^{k_2 n_2} \\ &= A_G(k_1, k_2) e^{j\theta_G(k_1, k_2)}, \end{aligned} \tag{2}$$

where $k_1 = -M_1, \cdots, M_1$, $k_2 = -M_2, \cdots, M_2$, $W_{N_1} = e^{-j\frac{2\pi}{N_1}}$, $W_{N_2} = e^{-j\frac{2\pi}{N_2}}$, and $\sum_{n_1, n_2}$ denotes $\sum_{n_1=-M_1}^{M_1} \sum_{n_2=-M_2}^{M_2}$. $A_F(k_1, k_2)$ and $A_G(k_1, k_2)$ are amplitude components and $\theta_F(k_1, k_2)$ and $\theta_G(k_1, k_2)$ are phase components. The normalized cross power spectrum $R_{FG}(k_1, k_2)$ is given by

$$\begin{aligned} R_{FG}(k_1, k_2) &= \frac{F(k_1, k_2)\overline{G(k_1, k_2)}}{\left|F(k_1, k_2)\overline{G(k_1, k_2)}\right|} \\ &= e^{j\theta(k_1, k_2)}, \end{aligned} \tag{3}$$

where $\overline{G(k_1, k_2)}$ is the complex conjugate of $G(k_1, k_2)$ and $\theta(k_1, k_2)$ denotes the phase difference $\theta_F(k_1, k_2) - \theta_G(k_1, k_2)$. The POC function $r_{fg}(n_1, n_2)$ is the 2D Inverse DFT (2D IDFT) of $R_{FG}(k_1, k_2)$ and is given by

$$r_{fg}(n_1, n_2) = \frac{1}{N_1 N_2} \sum_{k_1, k_2} R_{FG}(k_1, k_2) W_{N_1}^{-k_1 n_1} W_{N_2}^{-k_2 n_2}, \tag{4}$$

where $\sum_{k_1, k_2}$ denotes $\sum_{k_1=-M_1}^{M_1} \sum_{k_2=-M_2}^{M_2}$. When two images are similar, their POC function gives a distinct sharp peak. When two images are not similar, the peak drops significantly. The height of the peak gives a good similarity measure for image matching, and the location of the peak shows the translational displacement between the images.

We have also proposed a BLPOC (Band-Limited Phase-Only Correlation) function [11] dedicated to biometric authentication tasks. The idea to improve the matching performance is to eliminate meaningless high frequency components in the calculation of normalized cross power spectrum R_{FG} depending on the inherent frequency components of images. Assume that the ranges of the inherent frequency band are given by $k_1 = -K_1, \cdots, K_1$ and $k_2 = -K_2, \cdots, K_2$, where $0 \le K_1 \le M_1$ and $0 \le K_2 \le M_2$. Thus, the effective size of frequency spectrum is given by $L_1 = 2K_1 + 1$ and $L_2 = 2K_2 + 1$. The BLPOC function is given by

$$r_{fg}^{K_1 K_2}(n_1, n_2) = \frac{1}{L_1 L_2} {\sum_{k_1, k_2}}' R_{FG}(k_1, k_2) W_{L_1}^{-k_1 n_1} W_{L_2}^{-k_2 n_2}, \tag{5}$$

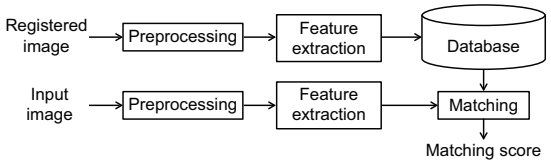

Figure 1. Flow diagram of biometric recognition system.

where $n_1 = -K_1, \cdots, K_1$, $n_2 = -K_2, \cdots, K_2$, and $\sum'_{k_1,k_2}$ denotes $\sum_{k_1=-K_1}^{K_1} \sum_{k_2=-K_2}^{K_2}$. Note that the maximum value of the correlation peak of the BLPOC function is always normalized to 1 and does not depend on L_1 and L_2.

2.2. Local Phase Features

Fig. 1 shows the general flow diagram of the biometric recognition system. In the preprocessing process, the position and illumination of images are often normalized according to type of the biometric trait. For example, in the case of face recognition, we detect the face region, extract feature points such as eyes, nose, mouth, etc., and then normalize the position of the face according to feature points. In the case of iris recognition, we detect the inner boundary between the iris and pupil and the outer boundary between the iris and sclera, and then unwrap the iris region to a normalized rectangular block of a fixed size using polar coordinate transformation. In the case of palmprint recognition, we extract the palm region of the fixed size from the hand image based on the location of the bottom of gaps between index and middle fingers and between ring and little fingers. Although the global transformation of the image can be normalized by the preprocessing process mentioned above, the nonlinear deformation inherent in each biometric trait may still remain. In order to achieve reliable biometric recognition, we have to extract features which can handle nonlinear deformation.

We employ local phase features extracted from multiscale image pyramids. Hierarchical features extracted from the registered image allow us to find corresponding local block images in the input image even for deformed images, since the nonlinear deformation is approximately represented by the minute translational displacement between local blocks. The fundamental algorithm has been proposed in Ref. [27]. This algorithm is designed for applications of computer vision to find correspondence between images with sub-pixel accuracy, and hence it is not always suitable for biometric recognition. In order to dedicate the hierarchical correspondence matching to biometric recognition, we employ 3 image layers with BLPOC-based local block matching as shown in Fig. 2. In the top layer, the global translation is aligned using the entire images. The images obtained after preprocessing may not be completely normalized, and hence may have global translation. In order to improve the accuracy of local block matching, we have to

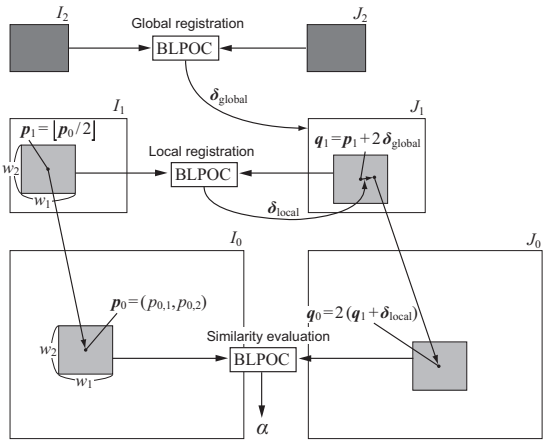

Figure 2. Hierarchical local block matching using BLPOC for biometric recognition.

align the global translational displacement in the top layer. In the middle layer, the local translation is aligned using the local block images. Focusing on local regions, image transformation such as scale, rotation, translation and nonlinear deformation can be considered as minute translations. By aligning local translation in this layer, we can handle nonlinear deformation of images. And finally, in the bottom (or original image) layer, the similarity between local blocks is evaluated by BLPOC.

The followings are detailed procedure for feature extraction and matching of hierarchical local phase features.

2.2.1 Feature Extraction

The hierarchical local phase features consist of the phase feature of the entire image in the top layer and local phase features of local block images in the middle and bottom layers. Local phase features in the middle and bottom layers are extracted according to the position of reference points. Fig. 3 shows an example of hierarchical local phase features extracted from an finger knuckle image. The feature extraction step consists of (i) reference point placement, (ii) hierarchical image generation and (iii) phase feature extraction.

(i) Reference point placement

The reference points are the center coordinate of each local phase feature. In this paper, we set the reference points in a reticular pattern. In the following, let the reference points be $\boldsymbol{p} = (p_1, p_2)$ $(= \boldsymbol{p}^0)$ and the registered image be I $(= I^0)$, respectively.

(ii) Hierarchical image generation

For $l = 1, 2$, we generate the l-th layer images $I^l(n_1, n_2)$ as follows:

$$I^l(n_1, n_2) = \frac{1}{4} \sum_{i_1=0}^{1} \sum_{i_2=0}^{1} I^{l-1}(2n_1 + i_1, 2n_2 + i_2). \quad (6)$$

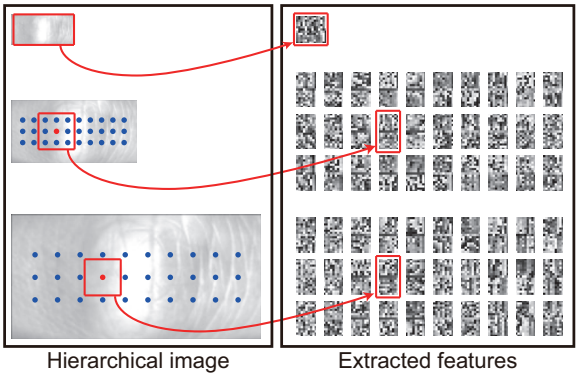

Figure 3. Example of feature extraction from a finger knuckle image, where "•" indicates the reference point.

Also, we calculate the coordinate $\boldsymbol{p}^1 = (p_1^1, p_2^1)$ corresponding to $\boldsymbol{p}^0$ on $I^1(n_1, n_2)$ as follows:

$$\boldsymbol{p}^1 = \left\lfloor \frac{1}{2}\boldsymbol{p}^0 \right\rfloor = \left(\left\lfloor \frac{1}{2}p_1^0 \right\rfloor, \left\lfloor \frac{1}{2}p_2^0 \right\rfloor \right). \quad (7)$$

(iii) Phase feature extraction

In the top layer, we calculate 2D DFT of I^2 and its phase components. In the middle and bottom layers, we extract $w_1 \times w_2$-pixel local block images with its center on $\boldsymbol{p}^1$ and $\boldsymbol{p}^0$ from I^1 and I^0, respectively. Then, we calculate 2D DFTs of all the local image blocks and their phase components. To reduce the size of hierarchical local phase features, we can eliminate the meaningless high frequency components which are not required for calculating the BLPOC function. We also reduce the size of phase information based on the symmetry property of DFT.

(iv) Phase quantization

A phase component $\phi(k_1, k_2)$ is generally represented by the real value between $-\pi$ and π. If the real-valued local phase features are stored into the database, the recognition system have to keep a large amount of registered data. To address the above problem, we reduce the amount of registered data by phase quantization. In this paper, we consider 4 types of phase quantization as shown in Fig. 4. Note that we select the range of quantization so that $e^{j\phi(k_1,k_2)}$ is always represented by the complex value, since we empirically confirm that the recognition performance is significantly dropped when $e^{j\phi(k_1,k_2)}$ is represented only by the real value.

2.2.2 Matching

The matching step consists of (i) hierarchical image generation of the input image, (ii) global image registration in the top layer, (iii) local image block registration in the middle layer, (iv) similarity evaluation in the bottom layer and (v) matching score calculation. Fig. 5 shows an example of matching between hierarchical local phase features in Fig. 3 and the input finger knuckle image.

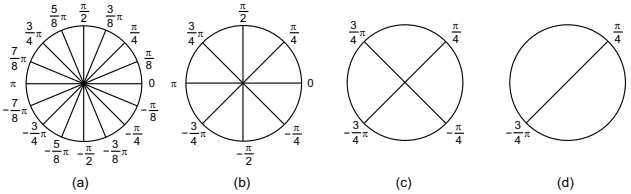

Figure 4. Range of phase quantization used in this paper: (a) 4 bit, (b) 3 bit, (c) 2 bit and (d) 1 bit

(i) Hierarchical image generation of the input image

Let J $(= J^0)$ be the input image and $\boldsymbol{q} = (q_1, q_2)$ $(= \boldsymbol{q}^0)$ be the corresponding points, respectively. For $l = 1, 2$, we generate the l-th layer images $J^l(n_1, n_2)$ as follows:

$$J^l(n_1, n_2) = \frac{1}{4}\sum_{i_1=0}^{1}\sum_{i_2=0}^{1} J^{l-1}(2n_1 + i_1, 2n_2 + i_2). \quad (8)$$

(ii) Global image registration in the top layer

In the top layer, we estimate the translational displacement between I^2 and J^2 using BLPOC. We denote the estimated global translations as $\boldsymbol{\delta}_{\mathrm{global}} = (\delta_{\mathrm{global},1}, \delta_{\mathrm{global},2})$.

(iii) Local image block registration in the middle layer

In the middle layer, we estimate the translational displacement between local block images of I^1 and J^1. We extract the $w_1 \times w_2$-pixel image blocks with its center on $\boldsymbol{q}^1 = \boldsymbol{p}^1 + 2\boldsymbol{\delta}_{\mathrm{global}}$ from J^1. Using BLPOC for each local block image pair of I^1 and J^1, we estimate the local translations $\boldsymbol{\delta}_{\mathrm{local}}$.

(iv) Similarity evaluation in the bottom layer

We evaluate the similarity between each local block image pair in the bottom layer. We extract the $w_1 \times w_2$-pixel local block images with its center on $\boldsymbol{q}^0 = 2(\boldsymbol{q}^1 + \boldsymbol{\delta}_{\mathrm{local}})$ from J^0. Then, we calculate the BLPOC function between each local block image pair of I^0 and J^0 and obtain the correlation peak value α.

(v) Matching score calculation

We evaluate the matching score between I and J according to the correlation peak values obtained in the step (iv). In this paper, we employ the matching score S defined by

$$S = \frac{N_{\mathrm{threshold}}}{N_{\mathrm{block}}}, \quad (9)$$

where $N_{\mathrm{threshold}}$ is the number of local image block pairs which peak values are higher than threshold th, and N_{block} is the number of local image block pairs.

3. Experiments and Discussion

In this section, we evaluate the performance of the proposed local features through a set of experiments in face recognition, palmprint recognition and finger knuckle recognition.

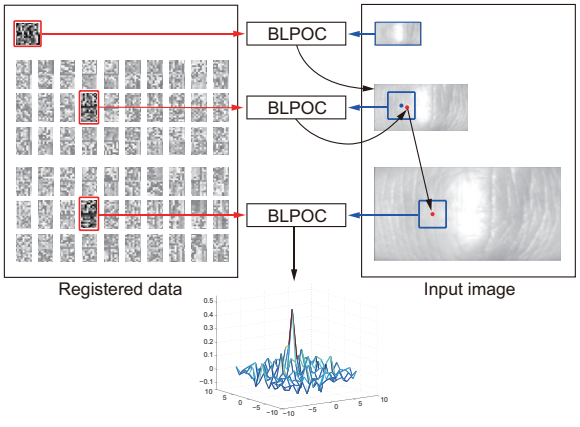

Figure 5. Example of matching between hierarchical local phase features in Fig. 3 and the input finger knuckle image.

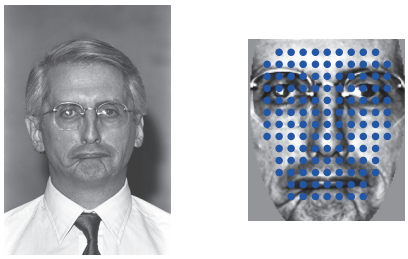

Figure 6. Example of a face image in FERET database: (a) original image and (b) the image after preprocessing, where "•" indicates the reference point for extracting a hierarchical local phase feature.

3.1. Face Recognition

To evaluate the performance in face recognition, we employ the CSU Face Identification Evaluation System [3] with the FERET database [24], where the recognition performance is evaluated by the Cumulative Match Characteristic (CMC) curve and the recognition rates of genuine pairs at rank 1. The FERET database contains 3,541 face images of 1,196 subjects. Fig. 6 shows an example of a face image and its normalized one. The images in the FERET database are organized into a gallery set *fa* and 4 probe sets such as *fb*, *fc*, *dup1* and *dup2*. The images in *fa* and *fb* set were taken in the same session with the same camera and illumination condition, but with different expression. The images in *fc* set were taken in the same session using the different camera and lighting. The images in *dup1* set were taken later in time. The images in *dup2* set which is a subset of *dup1* set were taken at least a year. Using the FERET database, we perform 4 experiments denoted by *fafb*, *fafc*, *dup1* and *dup2*. The parameters of the proposed algorithm are $w_1 = w_2 = 48$, $K_1/M_1 = K_2/M_2 = 0.5$, $th = 0.4$ and $N_{\text{block}} = 127$.

In the experiment, we compare 3 local features: SIFT [17], LBP [1] and the proposed local phase feature. Table 1 shows the recognition rate of genuine pairs at rank 1 for each local feature. The proposed method exhibits higher recognition rate than conventional methods for all the cases.

Table 1. Recognition rates of genuine pairs at rank 1 [%]

Algorithm	*fafb*	*fafc*	*dup1*	*dup2*
SIFT [17]	97	47	61	53
LBP (nonweighted) [1]	93	51	61	50
LBP (weighted) [1]	97	79	66	64
Proposed	99	100	88	89

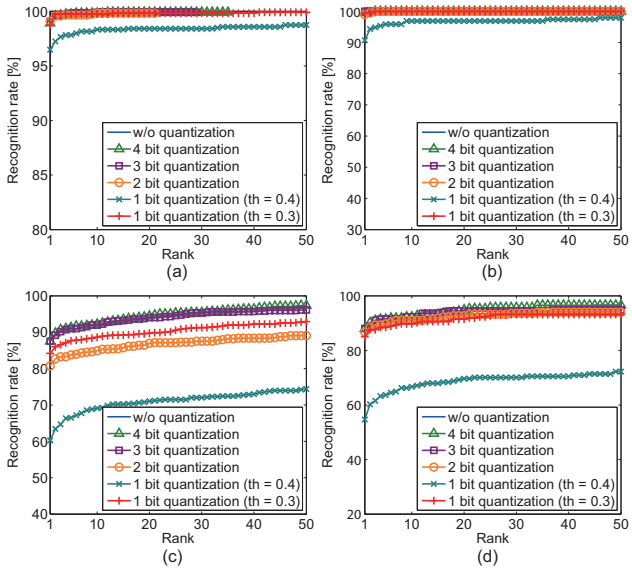

Figure 7. CMC curves for each quantization level using FERET database.

Table 2. Recognition rates of genuine pairs at rank 1 [%]

Quantization level	*fafb*	*fafc*	*dup1*	*dup2*
w/o	99	100	88	89
4 bit	99	99	88	88
3 bit	99	100	88	88
2 bit	99	99	86	87
1 bit ($th = 0.4$)	96	91	60	55
1 bit ($th = 0.3$)	99	99	84	85

We evaluate the impact of phase quantization in face recognition. Fig. 7 and Table 2 show CMC curves and the recognition rate of genuine pairs at rank 1 for the proposed method with and without phase quantization, respectively. In the case of 1-bit quantization, we compare 2 different thresholds th: one is the same as other quantization levels and the other one is lower. The recognition performance of the proposed method with phase quantization is comparable with that without phase quantization even for 1-bit phase quantization.

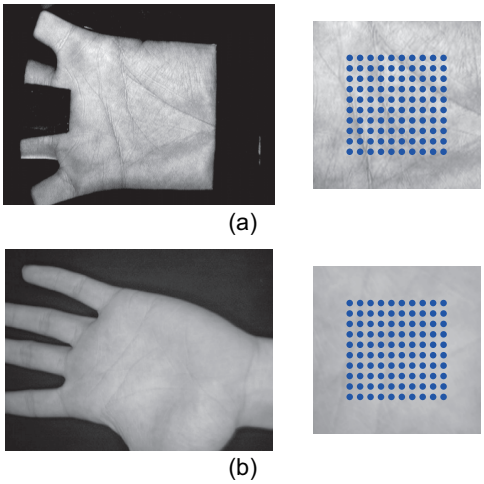

Figure 8. Example of a palmprint image in the database, where left is an original image and right is a normalized image and "•" on normalized image indicates reference point for extracting a hierarchical local phase features: (a) PolyU Palmprint database and (b) CASIA Palmprint database.

3.2. Palmprint Recognition

To evaluate the performance of palmprint recognition, we employ two palmprint databases: PolyU Palmprint database [1] and CASIA Palmprint database [2]. The PolyU Palmprint database consists of 7,752 contact palmprint images with 386 subjects. The number of genuine pairs is 74,068, while the number of imposter pairs is 29,968,808. The palmprint images in PolyU have only minute displacement since a hand is fixed on a system during the image acquisition as shown in Fig. 8 (a). The CASIA Palmprint database consists of 5,239 contactless palmprint images with left and right palm of 301 subjects. The number of genuine pairs is 20,584, while the number of imposter pairs is 13,700,357. The palmprint images in CASIA are deformed due to the contactless image acquisition as shown in Fig. 8 (b). We obtain the normalized palmprint images from all the images using the similar method described in Ref. [28] in advance, where the size of normalized images is 160×160 pixels. In this paper, the parameters of the proposed algorithm are $w_1 = w_2 = 48$, $K_1/M_1 = K_2/M_2 = 0.5$, $th = 0.3$ and $N_{\mathrm{block}} = 100$ as shown in Fig. 8.

We compare 4 local features: Competitive Code (CompCode) [12], Ordinal Code (OrdiCode) [25], Sparse Multiscale Competitive Code (SMCC) [33] and the proposed local phase feature. The recognition performance is evaluated by the Equal Error Rate (EER), which is defined as the error rate where the False Reject Rate (FRR) and False Accept Rate (FAR) are equal. Table 3 shows the summary of EERs for each method, where the EERs for the conventional algorithms are referred from Ref. [33]. As for PolyU, SMCC and the proposed method exhibit higher performance than other methods. As for CASIA, although the palmprint images in CASIA are deformed due to the contactless image acquisition, the performance of the proposed method is higher than all the other methods.

[1] http://www4.comp.polyu.edu.hk/~biometrics/

[2] http://www.cbsr.ia.ac.cn/english/PalmprintDatabases.asp

Table 3. EERs [%] for palmprint recognition

Algorithm	PolyU	CASIA
CompCode [33]	0.038	0.55
Ordinal Code [33]	0.104	0.84
SMCC [33]	0.014	0.48
Proposed	3.34×10^{-6}	0.07

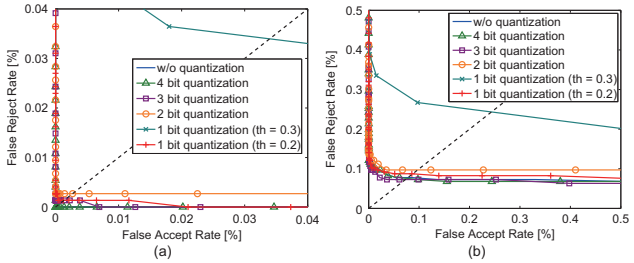

Figure 9. ROC curves for each quantization level: (a) PolyU and (b) CASIA.

Table 4. EERs [%] of each quantization level.

Quantization level	PolyU	CASIA
w/o	3.34×10^{-6}	0.0656
4 bit	5.00×10^{-6}	0.0695
3 bit	0.0011	0.0669
2 bit	0.0021	0.0822
1 bit ($th = 0.3$)	0.0272	0.1821
1 bit ($th = 0.2$)	0.0013	0.0866

We evaluate the impact of phase quantization in palmprint recognition. Fig. 9 and Table 4 show ROC curves and EERs for the proposed method with and without phase quantization, respectively. As is the case in face recognition, the recognition performance of the proposed method with phase quantization is comparable with that without phase quantization even for 1-bit phase quantization.

3.3. Finger Knuckle Recognition

To evaluate the performance in finger knuckle recognition, we employ the PolyU FKP database [3]. The PolyU FKP database consists of 7,920 images with 165 subjects

[3] http://www4.comp.polyu.edu.hk/~biometrics/FKP.htm

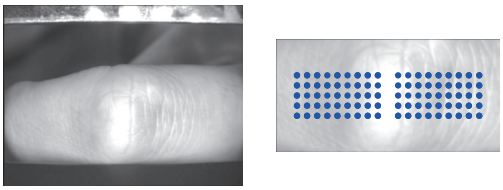

(a) (b)

Figure 10. Example of a finger knuckle image in the PolyU FKP database: (a) original image and (b) normalized image, where "•" indicates the reference point for extracting a hierarchical local phase feature.

Table 5. EERs [%] for finger knuckle recognition.

Algorithm	EER [%]
CompCode [32]	1.676
LGIC [32]	0.402
$LGIC_2$ [30]	0.358
Proposed	0.278

and 6 different images for each of the left index finger, the left middle finger, the right index finger and the right middle finger in 2 separate sessions. In the experiment, the images in the first session belong to the gallery set, while the images in the second session belong to the probe set, where each session consists of 660 (165×4) classes and 3,960 (660×6) images. The number of genuine pairs is 23,760 while the number of imposter pairs is 15,657,840 for this database. The PolyU FKP database provides the normalized finger knuckle images with 220×110 pixels. In the following experiments, we use the normalized finger knuckle images available in the database to evaluate the recognition performance. Fig. 10 shows an example of a finger knuckle image and its normalized one in the PolyU FKP database. The parameters of the proposed algorithm are $w_1 = w_2 = 48$, $K_1/M_1 = K_2/M_2 = 1$ in the top layer, $K_1/M_1 = K_2/M_2 = 0.5$ in other layers, $th = 0.3$ and $N_{\mathrm{block}} = 90$.

We compare 4 local features: CompCode [31], Local-Global Information Combination (LGIC) [32], $LGIC_2$ [30] and the proposed feature. The recognition performance is also evaluated by EER. Table 3 shows the summary of EERs for each method, where the EERs for the conventional algorithms are referred from Refs. [32, 30]. As a result, the proposed algorithm exhibits higher performance than all the other methods.

We evaluate the impact of phase quantization in finger knuckle recognition. Fig. 11 and Table 6 show ROC curves and EERs for the proposed method with and without phase quantization, respectively. As is the case in face and palmprint recognition, the recognition performance of the proposed method with phase quantization is comparable with that without phase quantization.

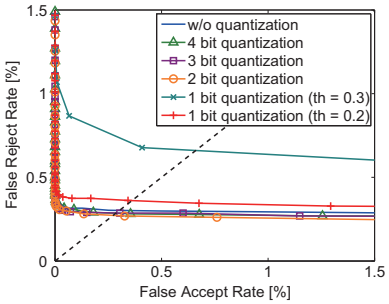

Figure 11. ROC curves for each quantization level.

Table 6. EERs [%] of each quantization level.

Quantization level	EER [%]
w/o	0.278
4 bit	0.235
3 bit	0.220
2 bit	0.208
1 bit ($th = 0.3$)	0.543
1 bit ($th = 0.2$)	0.352

Through a set of experiments for face recognition, palmprint recognition and finger knuckle recognition, we demonstrate that the hierarchical local phase features with phase quantization exhibit the efficient recognition performance and high versatility for biometric recognition.

3.4. Computation Time

The computation time of the proposed algorithm is evaluated by using MATLAB 7.14.0 (single thread use) on Intel Xeon X5690 (3.46 GHz). The computation time of feature extraction and matching is about 40∼60 msec. and about 70∼90 msec., respectively.

4. Conclusion

This paper has proposed the novel similarity measure technique using local phase features for biometric recognition. Through a set of experiments for face, palmprint and finger knuckle recognition, the proposed features exhibits efficient performance compared with the state-of-the-art conventional recognition algorithms. In future, we will apply the local phase features to other biometric traits and evaluate the versatility of local phase features. Also we will develop multibiometric systems based on local phase features and demonstrate the effectiveness of local phase features in multibiometric recognition problems.

References

[1] T. Ahonen, A. Hadid, and M. Pietikäinen. Face description with local binary patterns: Application to face recogni-

tion. *IEEE Trans. Pattern Analysis and Machine Intelligence*, 28(12):2037–2041, Dec. 2006.

[2] S. Aoyama, K. Ito, and T. Aoki. Finger-knuckle-print recognition using blpoc-based local block matching. *Proc. Asian Conf. Pattern Recognition*, pages 525–529, Nov. 2011.

[3] J. Beveridge, D. Bolme, B. Draper, and M. Texeira. The CSU face identification evaluation system. *Machine Vision and Applications*, 16:128–138, 2005.

[4] M. Bicego, A. Lagorio, E. Grosso, and M. Tistarelli. On the use of SIFT features for face authentication. *Proc. IEEE Computer Society Conf. Computer Vision and Pattern Recognition Workshops*, page 35, June 2006.

[5] C.-H. Chan, J. Kittler, and K. Messer. Multi-scale local binary pattern histograms for face recognition. *Lecture Notes in Computer Science (ICB2007)*, 4642:809–818, Aug. 2007.

[6] J. Chen and Y.-S. Moon. Using SIFT features in palmprint authentication. *Proc. Int'l Conf. Pattern Recognition*, pages 1–4, Dec. 2008.

[7] Q. Chen, M. Defrise, and F. Deconinck. Symmetric phase-only matched filtering of Fourier-Mellin transforms for image registration and recognition. *IEEE Trans. Pattern Analysis and Machine Intelligence*, 16(12):1156–1168, Dec. 1994.

[8] J. Daugman. High confidence visual recognition of persons by a test of statistical independence. *IEEE Trans. Pattern Analysis and Machine Intelligence*, 15(11):1148–1161, Nov. 1993.

[9] K. Ito, T. Aoki, H. Nakajima, K. Kobayashi, and T. Higuchi. A palmprint recognition algorithm using phase-only correlation. *IEICE Trans. Fundamentals*, E91-A(4):1023–1030, Apr. 2008.

[10] K. Ito, S. Iitsuka, and T. Aoki. A palmprint recognition algorithm using phase-based correspondence matching. *Proc. Int'l Conf. Image Processing*, pages 1977–1980, Nov. 2009.

[11] K. Ito, H. Nakajima, K. Kobayashi, T. Aoki, and T. Higuchi. A fingerprint matching algorithm using phase-only correlation. *IEICE Trans. Fundamentals*, E87-A(3):682–691, Mar. 2004.

[12] A. Kong and D. Zhang. Competitive coding scheme for palmprint verification. *Proc. Int'l Conf. Pattern Recognition*, 1:520–523, Dec. 2004.

[13] C. D. Kuglin and D. C. Hines. The phase correlation image alignment method. *Proc. Int'l Conf. Cybernetics and Society*, pages 163–165, 1975.

[14] A. Kumar. Can we use minor finger knuckle images to identify humans? *Proc. Int'l Conf. Biometrics: Theory, Applications and Systems*, pages 55–60, Sept. 2012.

[15] A. Kumar and Y. Zhou. Human identification using knucklecodes. *Proc. Int'l Conf. Biometrics: Theory, Applications and Systems*, pages 1–6, Sept. 2009.

[16] D. Lowe. Distinctive image features from scale-invariant keypoints. *Int'l J. Computer Vision*, 60(2):91–110, Jan. 2004.

[17] J. Luo, Y. Ma, E. Takikawa, S. Lao, and M. Kawade. Person-specific SIFT features for face recognition. *Proc. Int'l Conf. Acoustics, Speech and Signal Processing*, 2:II–593–II–596, Apr. 2007.

[18] G. K. O. Michael, T. Connie, and B. J. T. Andrew. Touch-less palm print biometrics: Novel design and implementation. *Image and Vision Computing*, 26:1551–1560, July 2008.

[19] K. Miyazawa, K. Ito, T. Aoki, K. Kobayashi, and H. Nakajima. An effective approach for iris recognition using phase-based image matching. *IEEE Trans. Pattern Analysis and Machine Intelligence*, 30(10):1741–1756, Oct. 2008.

[20] A. Morales, C. Travieso, M. Ferrer, and J. Alonso. Improved finger-knuckle-print authentication based on orientation enhancement. *IEEE Electronics Letters*, 47(6):380–381, Mar. 2011.

[21] L. Nanni and A. Lumini. Local binary patterns for a hybrid fingerprint matcher. *Pattern Recognition*, 41:3461–3466, Nov. 2008.

[22] T. Ojala, M. Pietikäinen, and Mäenpää. Multiresolution gray-scale and rotation invariant texture with local binary patterns. *IEEE Trans. Pattern Analysis and Machine Intelligence*, 24(7):971–987, July 2002.

[23] U. Park, S. Pankanti, and A. Jain. Fingerprint verification using SIFT features. *Proc. SPIE Defence and Security Symposium*, 6944, Mar. 2008.

[24] P. Phillips, H. Moon, S. Rizvi, and P. Rauss. The FERET evaluation methodology for face recognition algorithms. *IEEE Trans. Pattern Analysis Machine Intelligence*, 22(10):1090–1104, Oct. 2000.

[25] Z. Sun, T. Tan, Y. Wang, and S. Li. Ordinal palmprint represention for personal identification. *Proc. IEEE Computer Society Conf. Computer Vision and Pattern Recognition*, 1:279–284, June 2005.

[26] K. Takita, T. Aoki, Y. Sasaki, T. Higuchi, and K. Kobayashi. High-accuracy subpixel image registration based on phase-only correlation. *IEICE Trans. Fundamentals*, E86-A(8):1925–1934, Aug. 2003.

[27] K. Takita, M. A. Muquit, T. Aoki, and T. Higuchi. A sub-pixel correspondence search technique for computer vision applications. *IEICE Trans. Fundamentals*, E87-A(8):1913–1923, Aug. 2004.

[28] D. Zhang, W. Kong, J. You, and M. Wong. Online palmprint identification. *IEEE Trans. Pattern Analysis and Machine Intelligence*, 25(9):1041–1050, Sept. 2003.

[29] L. Zhang, L. Zhang, and D. Zhang. Finger-knuckle-print verification based on band-limited phase-only correlation. *Lecture Notes in Computer Science (CAIP2009)*, 5702:141–148, Sept. 2009.

[30] L. Zhang, L. Zhang, D. Zhang, and Z. Guo. Phase congruency induced local features for finger-knuckle-print recognition. *Pattern Recognition*, 45:2522–2531, July 2012.

[31] L. Zhang, L. Zhang, D. Zhang, and H. Zhu. Online finger-knuckle-print verification for personal authentication. *Pattern Recognition*, 43:2560–2571, July 2010.

[32] L. Zhang, L. Zhang, D. Zhang, and H. Zhu. Ensemble of local and global information for finger-knuckle-print recognition. *Pattern Recognition*, 44:1990–1998, Sept. 2011.

[33] W. Zuo, Z. Lin, Z. Guo, and D. Zhang. The multiscale competitive code via sparse representation for palmprint verification. *Proc. IEEE Computer Society Conf. Computer Vision and Pattern Recognition*, pages 2265–2272, June 2010.